EXPERIMENTAL ANALYSIS OF INSTABILITY PHENOMENA IN A HIGH-HEAD REVERSIBLE PUMP-TURBINE AT LARGE PARTIAL FLOW CONDITION

Pavesi G.[1*], Jun Yang[2], Cavazzini G.[1], Ardizzon G.[1]

[1]Department of Mechanical Engineering - University of Padova
Via Venezia 1 – 35131 Padova - Italy
giorgio.pavesi@unipd.it

[2] School of Energy and Power Engineering, University of Shanghai For Science and Technology
516 Jun Gong Road, Shanghai 200093, P.R.China
sandy198716@163.com

ABSTRACT

Growing environmental concerns, and the need for better power balancing and frequency control have increased attention in renewable energy sources, such as, the reversible pump-turbine which can provide both power generation and energy storage. Pump-turbine operation along the hump-shaped curve can lead to unusual increases in water pressure pulsations, which lead to machine vibrations.

Measurements of wall pressure in the stators were performed together with high-speed flow visualizations. Starting from the best efficiency point (BEP) and by decreasing the flowrate, a significant increase of the pressure fluctuations was observed mainly in the wicket gates channels. The analyses in frequency and time-frequency domains showed a rise of low frequency components. High-speed movies revealed a quite uniform flow pattern in the guide vanes channels at the normal operating range, whereas, the flow was highly disturbed by rotating stall passage at part load. The situation was more critical in the dump flow rate range, where backflow and vortices in the guide vanes channels developed during the stall cell passage.

NOMENCLATURE

B	Impeller or guide vane or return channel width	m
D	diameter	m
g	acceleration due to gravity	m/s^{-2}
Gxx	power pressure	bar^2
H	Head	m
n	rotational speed of the impeller	rpm
n_b	number of blades	-
$n_s = n\,Q^{0.5}/h^{0.75}$	specific speed	m$^{0.75}$s$^{-1.5}$
Q	flow rate	m^3 s^{-1}
$BPF = n_b\,n/60$	Blade Passage Frequency	Hz
$St = f/BPF$	Strouhal number	-
StF	Strouhal number related to a subtonal pressure pulsation (StF ≈ 0.6625)	-
StR	Strouhal number related to the impeller rotating frequency (StR ≈ 0.143)	-

---

* Corresponding Author Tel.: +39 049 827 6768; fax: +39 049 827 6785 *E-mail address*: giorgio.pavesi @unipd.it (Prof. Giorgio Pavesi)

StS	Strouhal number related to a subtonal pressure pulsation (StS ≈0.335)	-
α	angle	degree
β	angle	degree
η	efficiency	-
λ	guide vanes' azimuthally position	degree
$\omega_s = \pi n/30\, Q^{0.5}/(gH)^{0.75}$	dimensionless specific speed	-

Subscript

2	outlet impeller	b	blade
3	inlet guide vane	Des	Design
4	inlet return channel		

INTRODUCTION

In recent years, an increased interest in pump-turbines has been recognized in the market. The rapid availability of pumped storage schemes and the benefits to the power system by peak lopping, providing reserve and rapid response for frequency control are becoming of growing advantage (Henry J M et al., 2012).

The main advantage of hydro-storage power plants is based in its option to very quickly provide electrical energy to the grid when it is needed by the customers. In response to this demand it was requested to develop pump-turbines that are reliable in dynamic operation modes. In that context it is requested to develop pump-turbines that reliably stand dynamic operation modes, fast changes of the discharge rate by adjusting the variable guide vanes as well as fast changes from pump to turbine operation and vice versa.

Furthermore, the overall operating range of a pump-turbine should be well balanced. Stability limits should be positioned considerably away from the normal operating range in pump operation mode, and the turbine operation should allow fast synchronisation to the grid as well as a smooth power rise should be guaranteed by opening the guide vanes.

To enable smooth transient behaviour during rapid variations of energy level (output or consumption), and to allow very fast changing from the pump mode to the turbine mode and reversely, the stable operation in off-design, start-up and transient conditions is a key issue for pump-turbines. At off design conditions in pump mode, the wickets gates channel and the draft tube do not work properly and give awkward boundary conditions to the impeller, together with a strong fluid-dynamical interaction between rotor and stator parts (Yuekun Sun, et al., 2014, Hui Sun et al., 2013, Li W., 2012 and Rodriguez C G et al., 2014, Ch Gentner C et al., 2012). The flow features such as separation and recirculation occur severely in an unsteady manner. Non-rotating components of the turbine, such as guide vanes, stay vanes, head cover, draft tube cone, and also on the hydraulic system, especially the penstock may experience strong dynamic load and high cycle fatigue stress that may result in the propagation of cracks and the failure of the shear pin or the guide vanes stem.

Several experimental and numerical analyses have been carried out to identify a possible connection of unsteady flows and pressure fluctuations developing inside centrifugal pumps with runner/guide vane geometries and operating conditions.

Guo and Maruta (2005) investigated the onset of resonance phenomena as a consequence of the circumferential unevenness of the pressure fluctuations, whereas Rodriguez et al. (2007) presented an interesting theoretical method to predict and explain the possible harmonics that could appear in a pump-turbine as a consequence of the interaction between moving and stationary blades.

The frequency content of the pressure fluctuations was analysed both in frequency and in the time-frequency domains by Pavesi et al. (2008), Cavazzini et al. (2009) and Yang J et al., (2013), whose study presented a spectral analysis of the unsteady phenomena developing in a pump-turbine. Their analyses highlighted the existence of a rotating structure of pressure pulsations at the runner exit appearing and disappearing in time, having greater intensity at part loads. This strong rotor

stator interaction (RSI), at off-design conditions, resulted to be further emphasized in multi-stage pump-turbines in which a 'full-load-instability' (FLI) develops in the range from 60 to 90% of the design flow rate (Yang J et al., 2013) whereas Pavesi et al (2008) analyzed the influence of two rotational speed on the inception and evolution of the pressure instabilities.

Numerical analysis were carried out by Cavazzini G et al., (2011) identifying the pulsating onset of reserve flow cells in the runner, moving along the blade length and from one channel to another. This unsteady behaviour in the runner resulted to be associated with a perturbation of the wickets gates channel flow field, characterized by an unsteady flow rate migrations between passages and by unsteady flow jets.

Liu et al. [2012] investigated the hump characteristic of a pump turbine based on an improved cavitation model, and the calculation results are in agreement with the experimental data. Braun [2005] carried out calculations for the flow distribution in pump mode and an head discharge curve was obtained. The results showed that there was strong vortex between the guide vanes and flow became worse when entering the hump region. Yan [2010] obtained the same fluctuation results as the testing in the vaneless region by using compressible model. Iino [2004] considered that the hump characteristic was related to complex vortex structure in the runner inlet and centre region of the tandem cascade through simulation and experimental investigation.

More recently, Li Deyou et al (2015) focused the numerical analyses into the hump region trying to correlate the hump characteristics to the vortex motion in the tandem cascade.

Numerical analysis were also carried out by Gentner et al. (2012) highlighting the dependence of the flow behaviour in the head drop from the specific speed of the pump-turbine.

The results of both experimental and numerical analyses highlighted the existence of a spatial fluctuation pattern concentrated close to the runner exit, whose fluctuations levels increases at off-design conditions.

Even though these studies have allowed to obtain interesting information on the unstable behaviour of pump-turbines, to solve instability problems and to significantly enlarge the working range of pump-turbine, an in-depth understanding of the unsteady flow mechanism at hump zone is crucial for the production stabilization.

The aim of this investigation is to analyse the characteristics of the instabilities of a two stages reversible-pump turbine operating in pump-mode and to study the development of the unsteady phenomena. The experimental research included the dynamic pressure measurements and high-speed flow visualizations from design to part flow rate. The analysis of pressure fluctuations were conducted both in frequency and time frequency domains and the flow visualization was focused in the wickets gates and in return channels.

EXPERIMENTAL SET-UP

The experimental study was carried out in the test rig for turbines and pumps at the Department of Industrial Engineering of the University of Padova.

The accuracy that can be achieved in the calculation of the efficiency and speed of the machines was 0.2% and ±0.5 rpm respectively. The calibration of the instruments was performed on site. The pump-turbine model was the low-pressure stage of a two stages $n_s = 37.6$ $m^{0.75}s^{-1}$. (dimensionless design specific speed $\omega_s = 0.71$) pump-turbine with a seven 3D backward swept blades with a discharge angle of 26.5°runner (Fig. 1).

Refeeding channels were used to guide
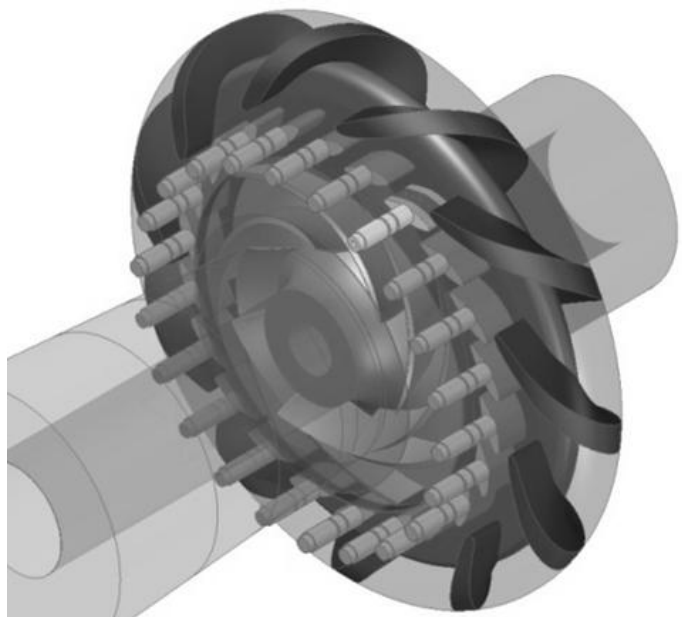
Fig. 1 3D scheme of the tested configuration.

the flow that leaves the impeller to the inlet of the subsequent channel. The channels were made up of twenty two adjustable guide-diffuser vanes and eleven continuous vanes. The guide-diffuser allows continuous and independent adjustment of the vane angle and of relative azimuthally position with the return channel vanes. The relative azimuthally position of the guides' vanes was fixed rotating the system of 8 degrees from the face to face configuration (reference position with $\lambda=0°$).

Geometry characteristics of the tested pump-turbine were listed in table 1.

Fig. 2 shows the gray guide vane and the return vane where the unsteady pressure was measured at the mid-height by 12 piezoresistive transducers Kulite XCL-072 (sensitivity of about 29.3 mV/bar), which were faced mounted. Details of this configuration and of the complete machine geometry can be found in Yang J et al., (2013).

The pressure signals were analyzed in both the frequency domain and the time–frequency domains (Torrence C and Compo G, 1998, Farge M., 1992) to identify and characterize the unsteady phenomena in the saddle region. The power spectra were computed by partitioning each time signal into 2^8 segments of 2^{10} samples with no overlapping, filtered with a Hanning window for avoiding aliasing and leakage errors. The frequency resolution was 0.125Hz. To determine the non-linear and linear components in the frequency domain, bispectrum analysis was carried on in this paper (Rosenblatt M and Van Ness J W., 1965).

To allow high-speed flow visualizations between stay vanes and guide vanes, the casing was manufactured in Plexiglas. A Photron FASTCAM PCI digital camera was used and the video camera recorded images at resolution 512×512 pixels with a frame rate 10000fps and a shutter 1/10000. Two tungsten halogen bulbs with 1000W were equipped to provide the light of the scene. Needle valves were employed to control the amount of injected air throughout holes of 0.5 mm diameter located in the mid span of the guide and return channel vanes located in the same positions of the pressure transducers, shown in Fig. 2. The injection pressure was maintained at a value slightly above the mean pressure at the injection location.

Table 1 Geometry characteristics and performance parameters of the tested pump-turbine.

Impeller data				
D_2 (mm)	B_2 (mm)	n_b	$\beta_{2b}(°)$	ϕ_{Des}
400	40	7	26.5	0.125
Guide vanes data				
D_3 (mm)	B_3 (mm)	n_b	α_{3b} (°)	$\lambda(°)$
410	40	22	10÷30	-8÷8
Return channel vanes data				
D_4 (mm)	B_4 (mm)	n_b	α_{4b} (°)	
516	40	11	30	
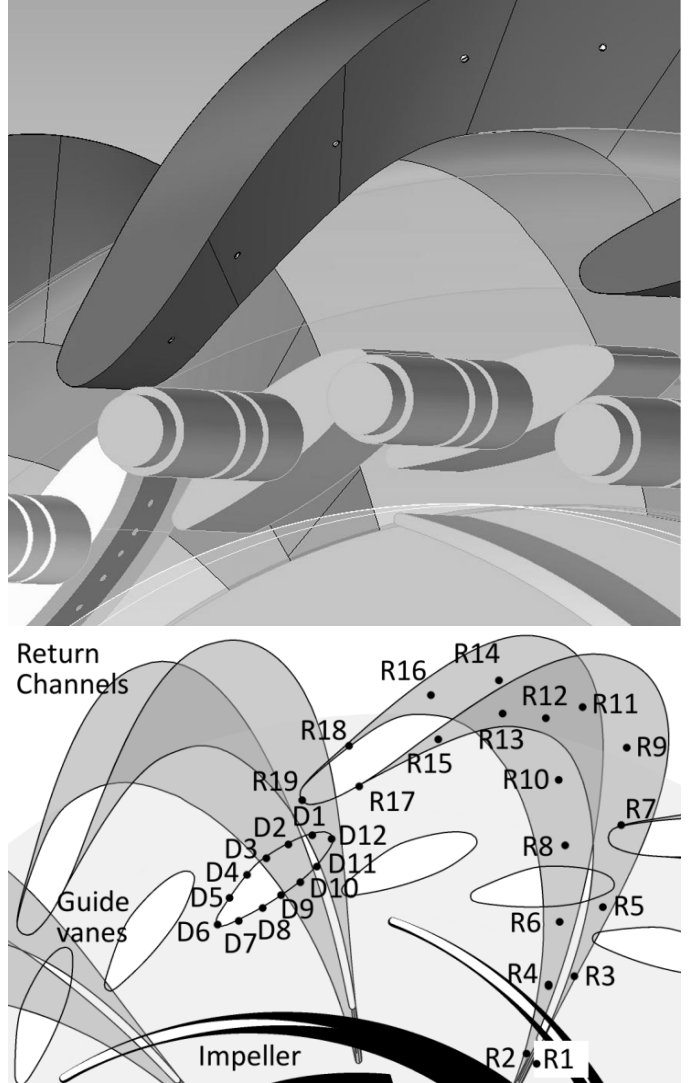
Fig. 2 Detail and sketch of the tested configuration ($\lambda=8°$) with the distribution of monitor points.

RESULTS

The characteristics, evaluated in accordance with ISO standards, show slightly hump-type instabilities behaviour between $Q/Q_{Des} \approx 0.45$ to 0.70 (Figure 3). Below $Q/Q_{Des} \approx 0.40$ the characteristic raised due to the effect of fully developed inlet recirculation. In the hump-type instability the data showed a limited repeatability. Consequently, the operational points were tested to see if increasing or decreasing Q might affect the outcome of the Fourier transform. The result was that the Fourier transforms were the same.
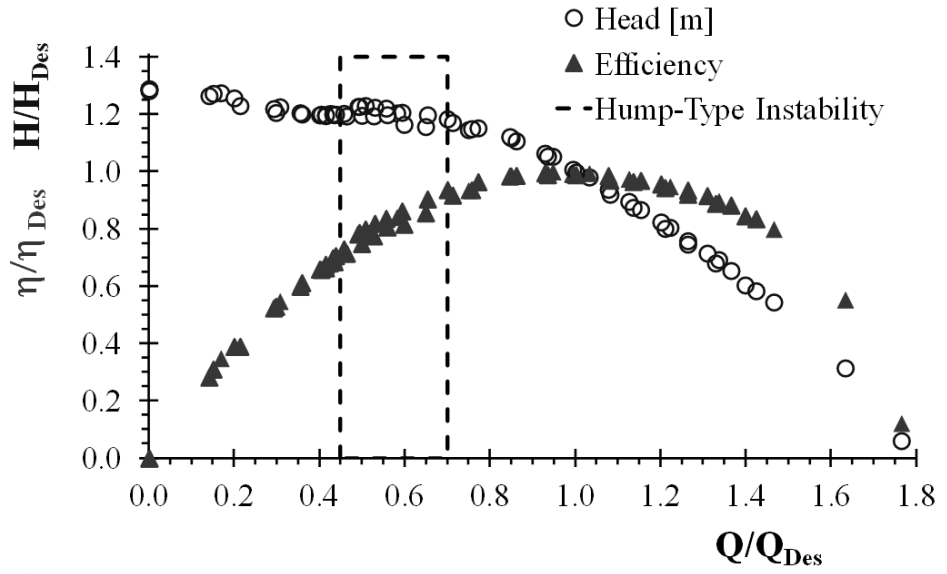
Fig. 3 Experimental pump characteristics.

To identify the flow structures into the instability zone, high-speed visualizations were made with the help of air bubbles injection in the guide and return vanes from the design flow rate, to the instability flow rate. The motion of air bubbles was theoretically analyzed for a radial pomp by Minemura and Murakami (1980). They solved the equation of motion for air bubbles in the flow field including the effects of the drag force and slip, density differences between the phases and inertia force. By comparing their results to the experimental data, they demonstrated that the bubble motion within the impeller is controlled by the corresponding drag force and the pressure gradient around the bubble. The tendency that bubbles deviate from the streamlines of liquid water raises with increasing bubble diameter.

Until the dimension of the bubbles were smaller than about 1 mm diameter, in the post process procedure it was assumed that air bubbles follow the streamlines with almost no effect on the flow itself.

Fig. 4 illustrates arbitrary instantaneous captures of the flow pattern in the guide vanes region for conditions around the design flow rate. The trajectory of air bubbles is quite straight inside the guide vanes channel with negligible longitudinally unsteadiness

(a) 1.06 Q_{Des} (b) 1.00 Q_{Des}

(c) 0.80 Q_{Des} (d) 0.70 Q_{Des}
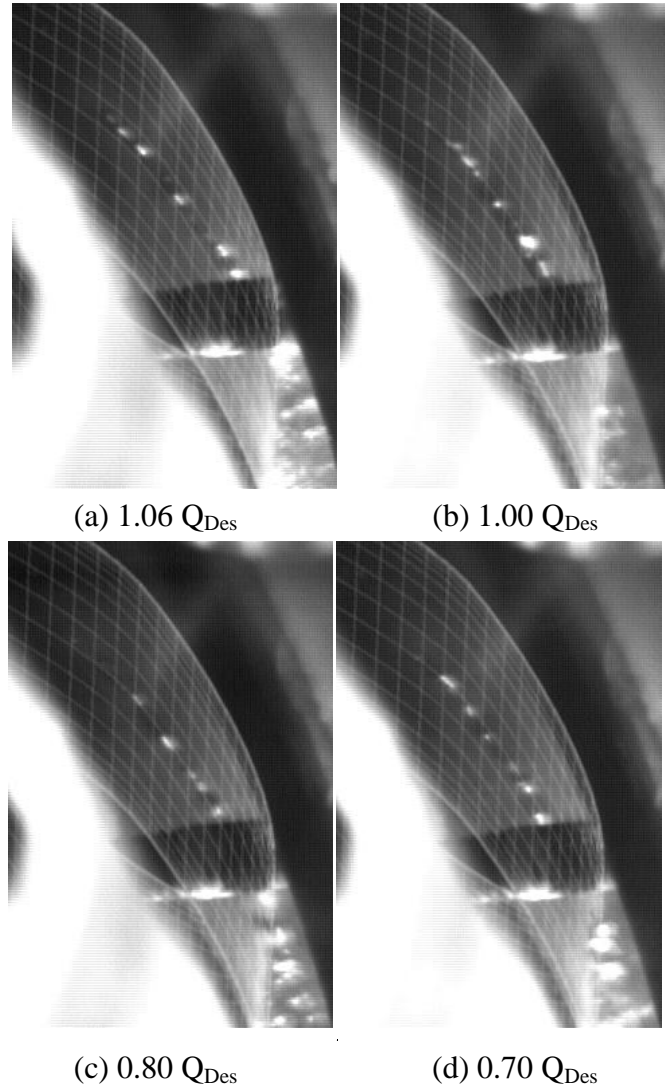
Fig. 4 Frames obtained by high speed camera at different flow rate in the wickets gates channel.

and slightly unstable in the wake of the neighbouring return vanes.

In the return vane channel, the bubbles blown out from a hole on the suction side were rapidly scattered forming puffs of bubbles. The bubbles flow pattern was close to the guide vane suction upper side (Fig. 5) along the dotted line. Moreover a reverse flow volume was present in the corner between the vane suction side and the U-Turn hub (dot line in central region in Fig. 5) The bubbles, blown out, were partially absorbed by the reverse flow and moved inside it in a cyclic path showing a pulsating oscillation. By the use of a stroboscopic light this recirculation, showed a pulsating oscillation equal to the impeller rotating frequency (StR=0.143).
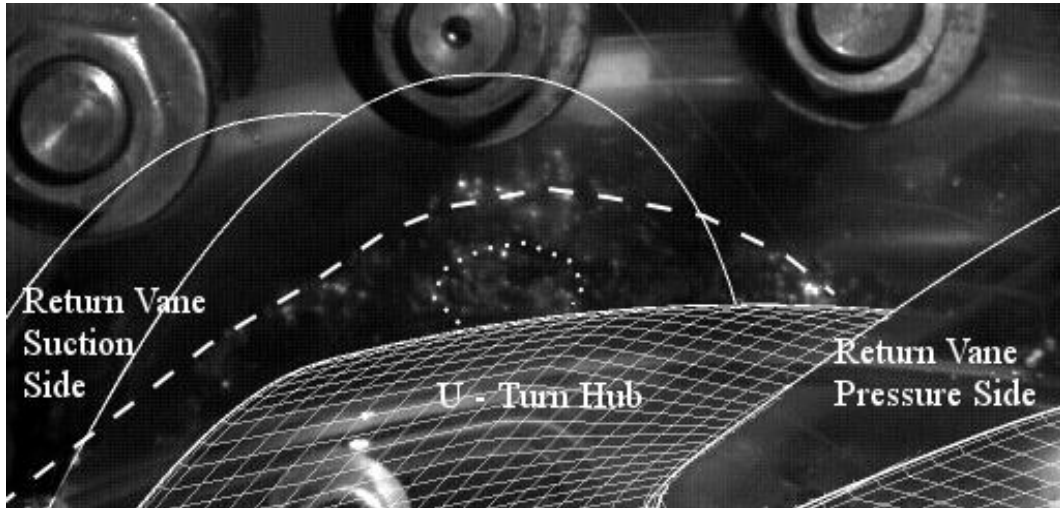
Fig. 5 Frame obtained by high speed camera in return channel at 1.06 Q/Q_Des
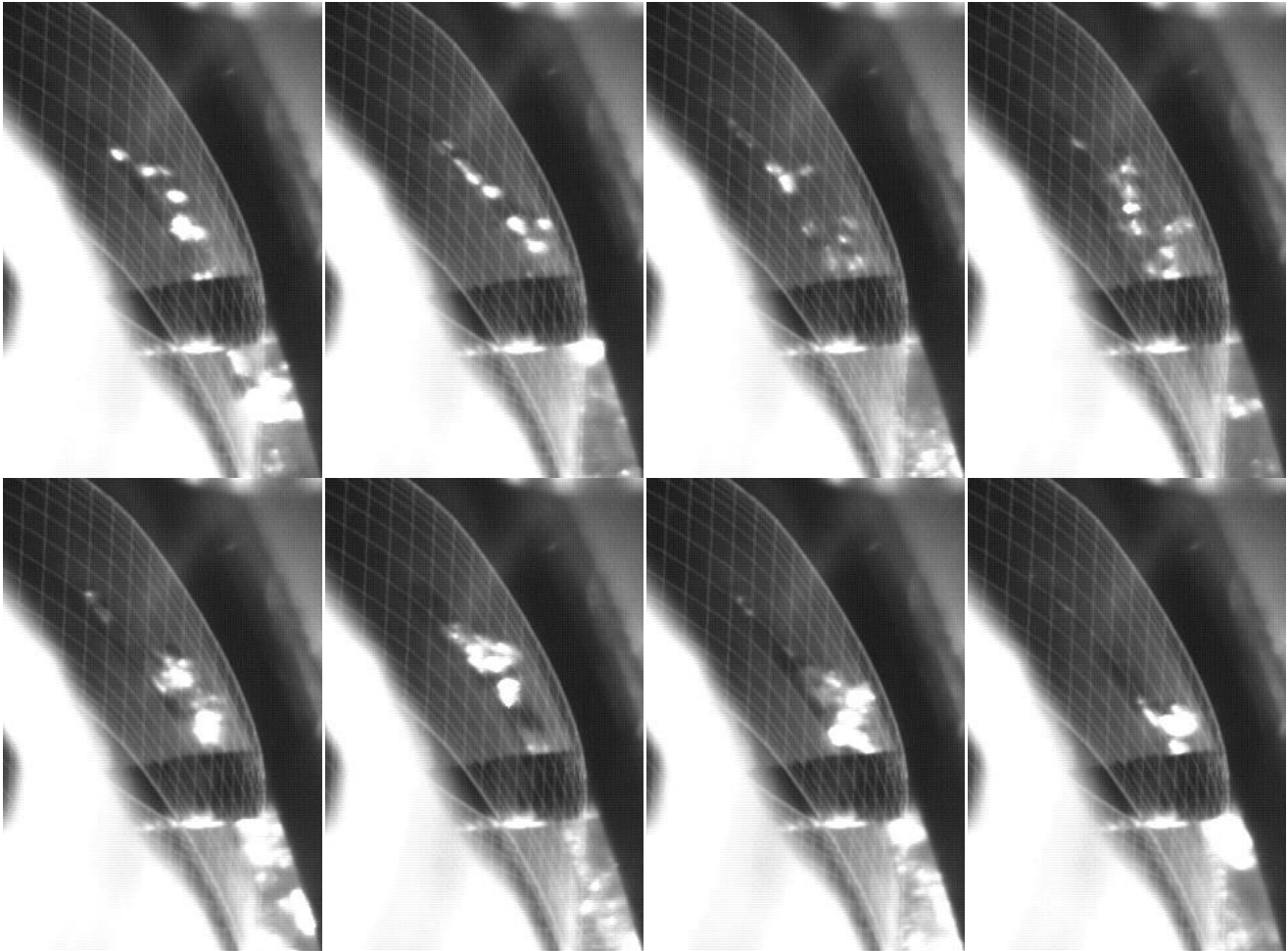
Fig. 6 Frames sequence obtained by high speed camera at $0.63Q_{Des}$ in the wickets gates channel.

Reducing the flow rate below 0.70 Q_{Des}, the flow becomes more disturbed, as evidenced by the scatter of air bubbles. At the beginning, the bubbles moved along the guide vane surface with random slowing down and restarting or rapid lateral shifting (Fig. 6). With the reduction of the flow rate, the frequency of the pulsations increased and a flow separation began to appear around the trailing edge and gradually extended along the wickets gates channel.

With a further flow rate reduction, the flow became more unstable. At flow rate below about 0.60 Q/Q_{Des}, the air injected through the hole of the vane gate was found periodically to move back toward the impeller and part of injected air was found upstream to the injection site, suggesting the occurrence of backflow, as shown in Fig. 7.

According to Fig. 7, at low discharge operating condition, a stall cell travels with the impeller at a constant sub-synchronous speed and induces the same pressure fluctuation amplitude in the whole vaned ring. Vortices and backflow dominate the flow pattern. Once the rotating stall passed, the flow returns step by step to a uniform pattern.

Numerical analyses (Pavesi G. et al., 2014) confirmed these remarks showing the appearance of five part span stall in the diffuser at the lower flow rate. Three stall

Fig. 7 Frames sequence obtained by high speed camera at 0.58 Q_{Des} in the wickets gates channel.

cells developed from the hub up to less than 20% of the diffuser width, one from the shroud to the mid span and only one showed a stable full span configuration.
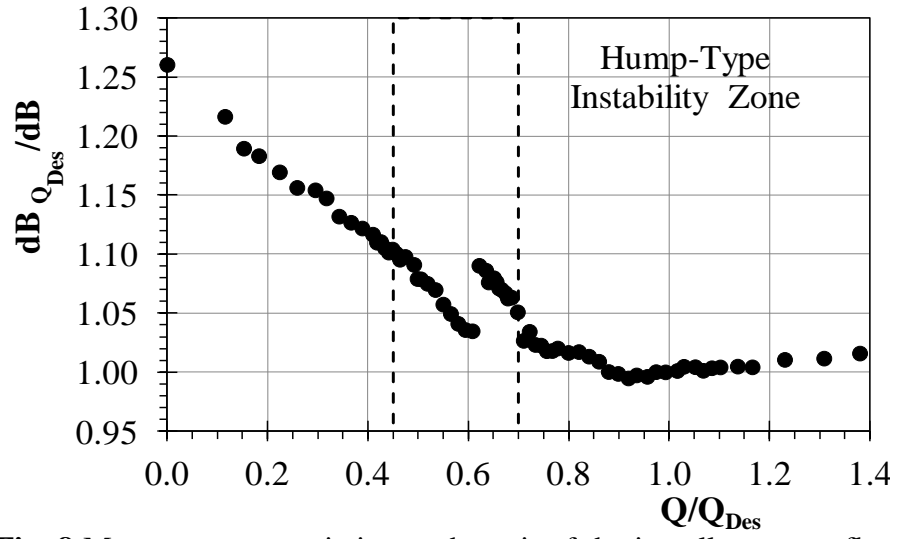
The mean pressure variation measured in the vaneless gap at the impeller outlet is shown versus the flow rate in figure 8. The mean pressure fluctuation shows a slight monotone increase for the flow rate, not far from the design flow rate and a sharp increase when the flow rate diminishes below the critical value $Q/Q_{Des} \approx 0.7$ that is the same flow rate value where the head characteristic was observed unstable and the high speed visualization showed the first unsteadiness (fig. 6). Moreover, the mean pressure shows a discontinuity when the flow field shows a change from random instabilities (fig. 6) up the appearance of stall cells (fig. 7).

The pressure signals frequency analyses showed peaks at the blade passage frequency (BPF, St=1), the impeller rotating frequency (StR ≈0.143), but also two other frequency peaks (figs 9 and 10). The main one at StF ≈0.6625 was observed in the flow interval $Q/Q_{Des} \approx 0.37$ to 1.19, the second one at StS ≈0.335 was observed in the flow interval $Q/Q_{Des} \approx 0.45$ to 0.75.

For flow rates greater than about 0.7 Q_{Des} the pressure fluctuation in the wickets gates channel shows peaks at the blade passage frequency (fig. 11), especially on the side faced to the impeller, at the impeller rotating frequency (StR ≈0.143), a little more evident on the side faced to the return channels, and in many other subtonal frequency peaks (fig. 11).

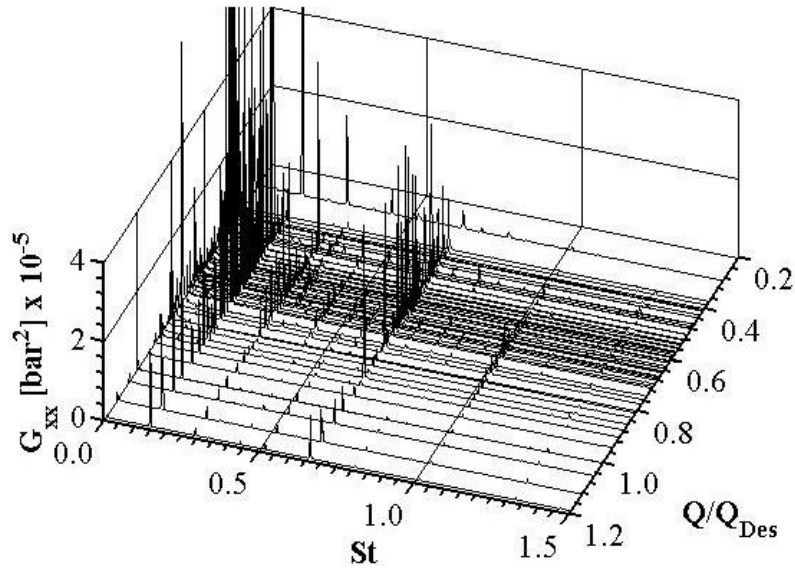**Fig. 8** Mean pressure variation at the exit of the impeller versus flow rate.
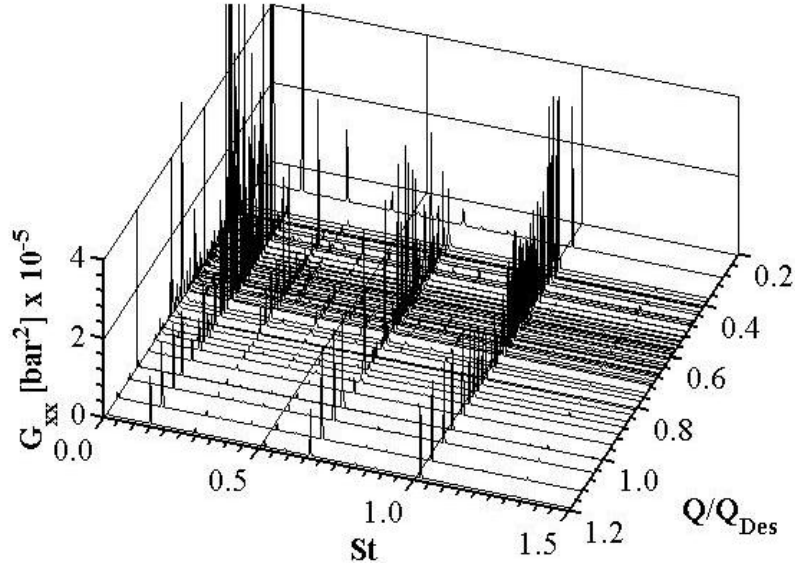
Fig. 9 Power pressure at the leading edge guide vane versus flow rate.

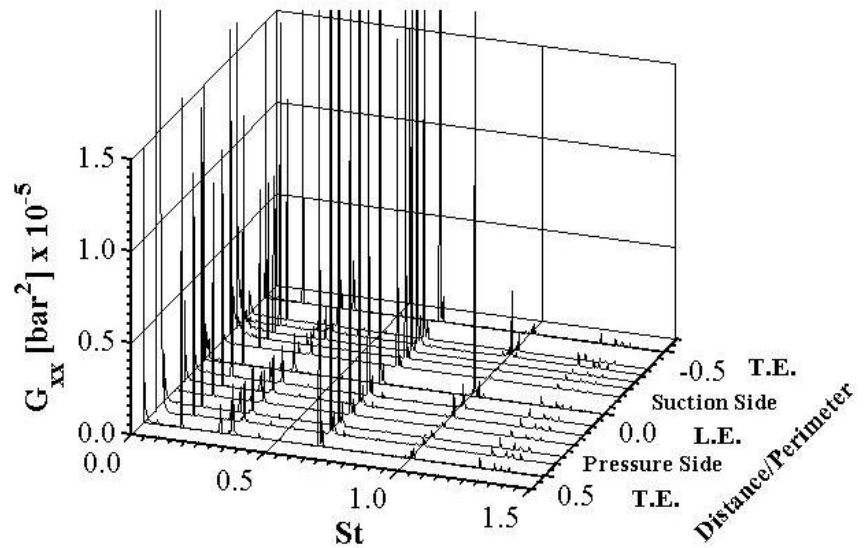**Fig. 10** Power pressure at the trailing edge guide vane versus flow rate.

The high order analyses highlighted that the measured pressure fluctuations were due to the non linear interaction between the blade passage frequency (St=1), the impeller passage frequency (StR≈0.143) and the subtonal frequency StF≈0.6625 (Fig. 12).

The impeller passage frequency shows higher coherence and intensity in the volume downstream the guide vanes and in the area close to the corner between the vane suction side and the U-Turn hub. This is consistent with the reverse flow volume shown in the corner by the air injection and its spin velocity. Moreover, on the back side of the return channel at all the flow rates, stagnant water persists in a zone close to the hub and the suction blade side. The air bubbles blew out in this area moved stochastically inside, up to the moment when all them are swept away with a frequency equal to StR (Yang et al (2015)).

Also, the subtonal frequency StF≈0.6625 was found to be related to a pressure fluctuation quite permanently present in the return channel. The air that blew on the guide vane suction side (Fig. 5) was rapidly scattered forming puffs of bubbles due to transversal flow and the frequency of the bubbles clouds was consistent with StF ≈ 0.6625.

A further reduction of the flow rate produce an increase of the overall power pressure intensity (fig. 8). Moreover, the number of the frequency peaks measured (fig. 13) and the intense non linear interaction between the aforesaid frequency in the gap between the impeller and the wicked vanes (fig. 14) increased.

The unsteady pattern in return channel strengthened, emphasizing a little its characteristic frequency StF ≈ 0.6625. But the more relevant effects

Fig. 11 Power pressure at the design flow rate along the guide vane surface.
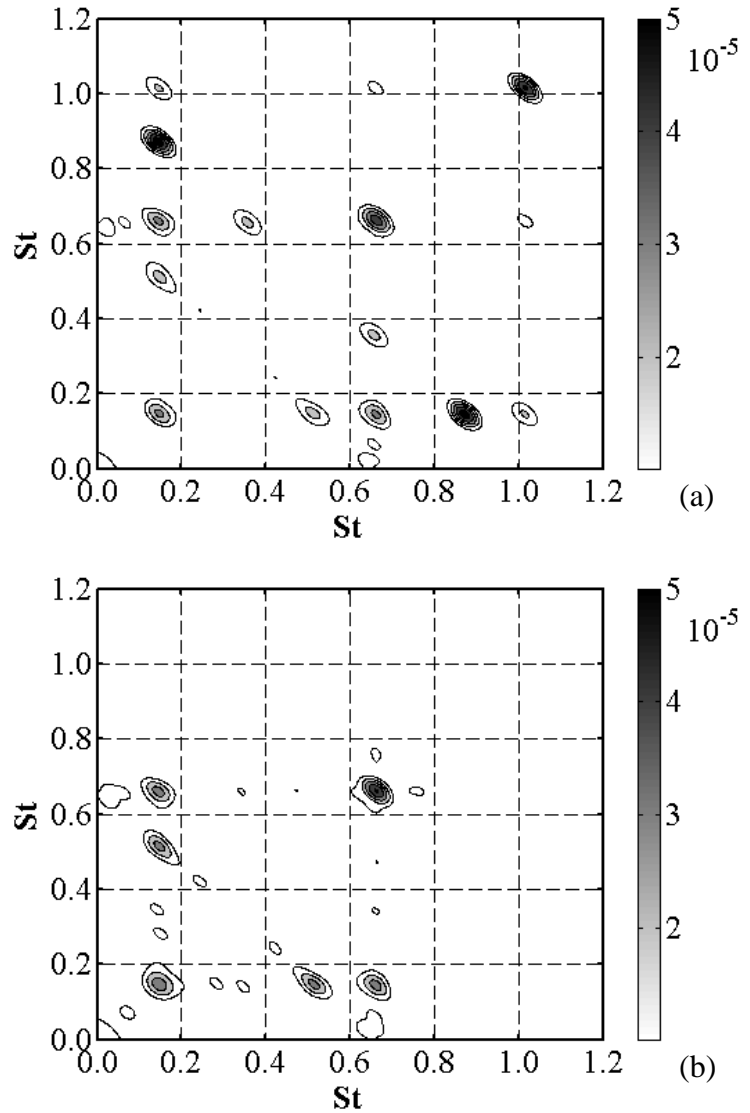
Fig. 12 Pressure Bispectrum at leading (a) and trailing (b) wickets gates channel edge at Q_{Des}

9

were related to the frequency StS≈0.335 (Fig. 14). The crosswise unstable, highlighted by the frames sequence in Fig. 6, was related to the boundary layer separation and stall in the wickets gates channel and was noticed with a frequency very close to StS.

When the flowrate was reduced below 0.60 Q_{Des} the effect of StS progressively disappears (Figs. 15 and 16). The incidental presence of amplitude at StS ≈ 0.335 is due to the nonlinear interaction between the components BPF and StF and it is not as a fundamental frequency (Fig. 16).

The existence of this fluid-dynamical unsteadiness was confirmed by the time-frequency analyses carried out at all the flow rates. In the instabilities zone, the power of the pressure pulsation of StF and StS gradually increases with the decrease of flowrate up to 0.60 Q_{Des}. Fig. 17 shows the wavelets at 0.62, 0.60 and 0.58 Q/Q_{Des}. The low frequency component StS presents a non constant pulsating value at 0.62 and 0.60 Q_{Des} while disappears at Q/Q_{Des} lower than 0.58.

For flow rates lower than the instability region, the periodic stall/back flow inside the wickets gates channel disappeared. The bubbles path analyses show only vortexes which intensity and structure that changed stochastically.

CONCLUSIONS

Experimental analyses were carried out on a low specific speed pump-turbine, operating at full and part load conditions on pump mode to study the characteristics and the development of the unsteady phenomena into bump-instabilities region. Both the pressure variation in time and frequency domains and high-speed flow visualizations were used to analyse the flow field mainly in
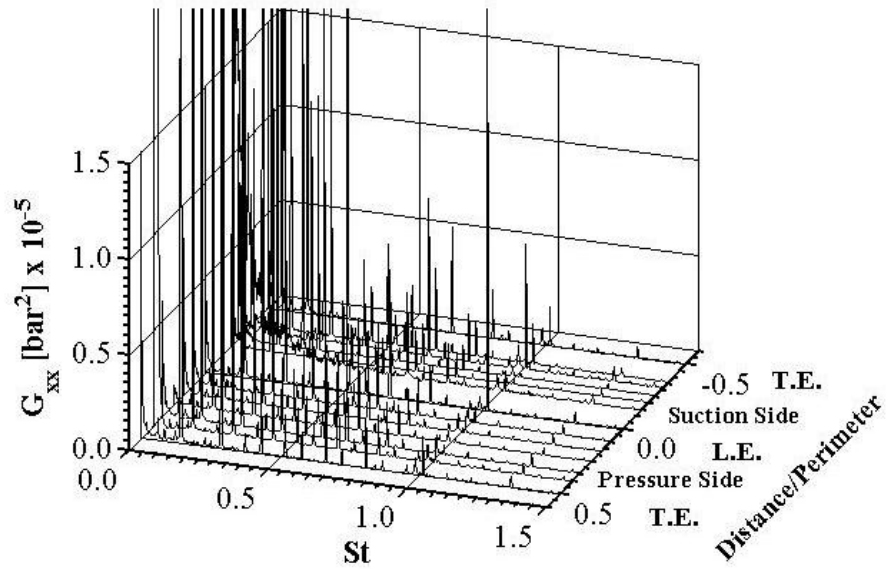
Fig. 13 Power pressure at 0.63Q_{Des} along the guide vane surface.
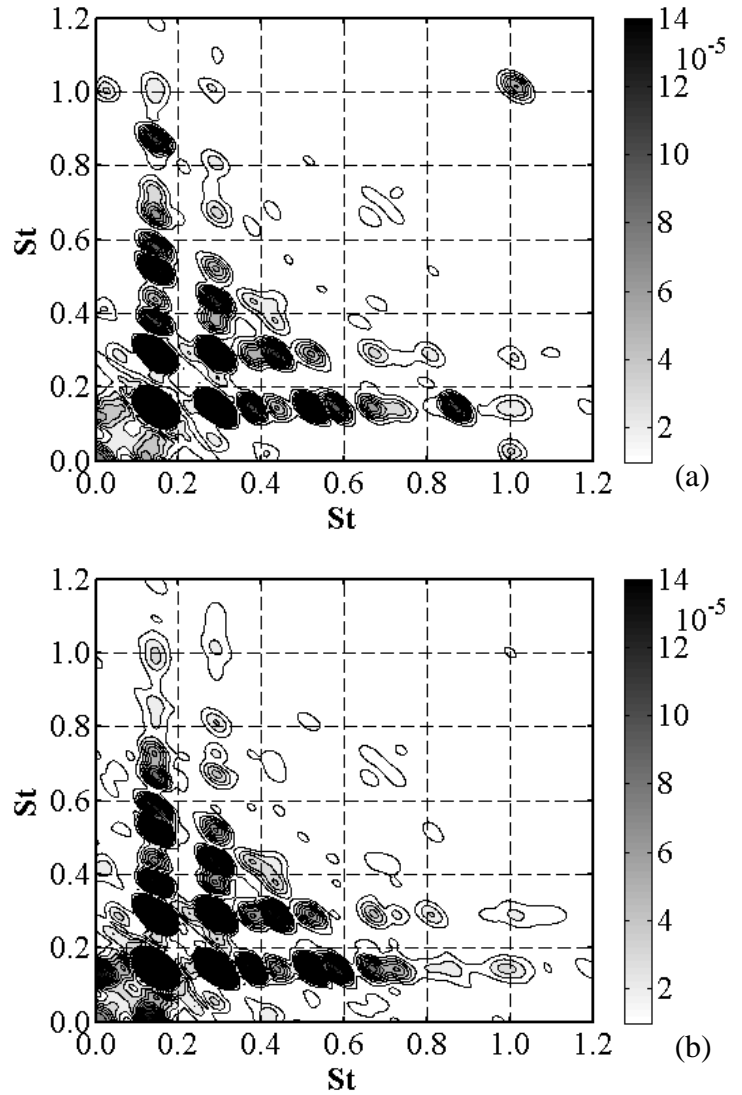
Fig. 14 Pressure Bispectrum at leading (a) and trailing (b) wickets gates channel edge at 0.63 Q_{Des}

the instability region from 0.45 to 0.70 Q/Q_{Des}.

Two different unsteady patterns were highlighted coherently by both spectral and bispectral analysis of the pressure data and high-speed flow visualization. When the flow rate decreased below the design flow rate, the back flow volume in the return channel moved along the suction side, extending towards the back side direction. The unsteady pattern in return channel strengthened emphasizing its characteristic frequency $StF \approx 0.6625$ with the flow rate decreasing.

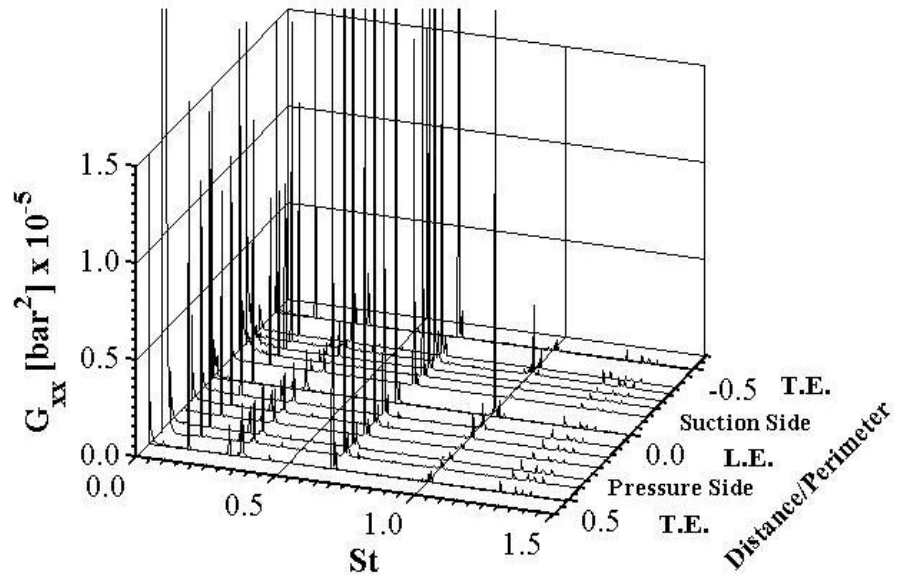**Fig. 15** Power pressure at 0.58 Q_{Des} along the guide vane surface.

At lower flow rate the flow field into the wickets gates channel manifested a full three-dimensional flow structure. This disturbance was related to the boundary layer separation and stall in the guide vane and was noticed with a frequency very close to $StS \approx 0.335$.

The high-speed camera results highlighted that the second unsteady perturbation ($StS \approx 0.335$) is coupled with an unsteady three-dimensional pattern into the wickets gates channels.
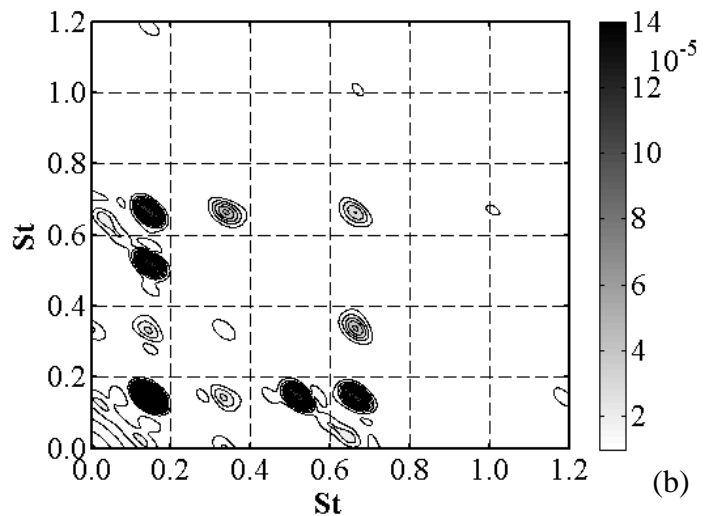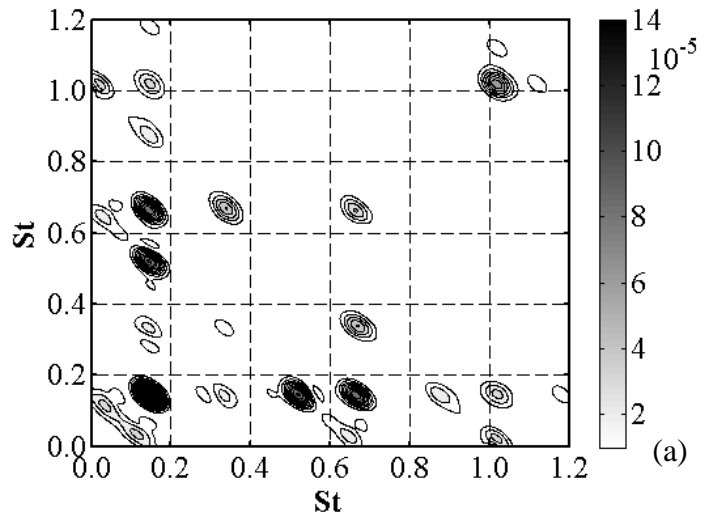
For flow rate lower than the instability region, the periodic stall/back flow inside the wickets gates channel disappeared. The bubbles path analyses show only vortexes with intensity and structure that changed stochastically.

REFERENCES

[1] Braun O, Kueny JL, Avella F. (2005) Numerical analysis of flow phenomena related to the unstable energy-discharge characteristic of a pump-turbine in pump mode. In: Proceedings of 2005 ASME fluids engineering division summer meeting and exhibition, Houston, USA; 2005.

[2] Cavazzini G., Pavesi G., Ardizzon G., Dupont P., Coudert S., Caignaert G., Bois G. (2009) Analysis of the rotor-
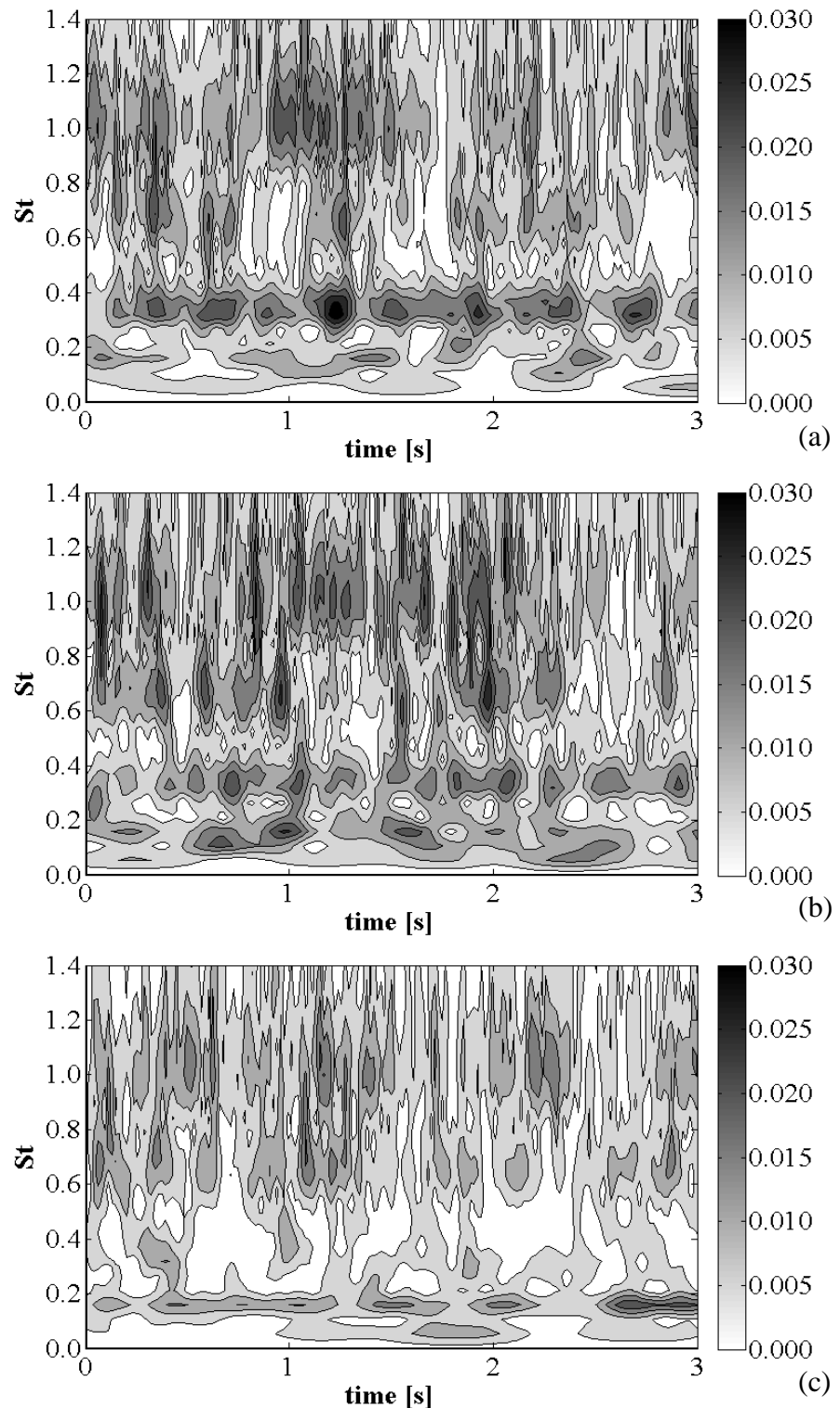
Fig. 16 Pressure Bispectrum at leading (a) and trailing (b) wickets gates channel edge at 0.58 Q_{Des}

stator interaction in a radial flow pump. La Houille Blanche, Revue Internationale de l'eau, 2009, 5, pp. 141–151, DOI 10.1051/lhb/2009067

[3] Cavazzini G., Pavesi G., Ardizzon G. (2011) Pressure instabilities in a vaned centrifugal pump, Proceedings of the Institution of Mechanical Engineers, Part A: Journal of Power and Energy, 225(7), pp. 930-939

[4] Farge M (1992) Wavelet transforms and their application to turbulence. Annu. Rev. Fluid Mech. 24, pp. 395–457.

[5] Gentner C., Sallaberger M., Widmer C., Barun O., Staubli T. (2012) Analysis of unstable operation of pump turbines and how to avoid it, HYDRO 2012 Innovative Approaches to Global Challenges, 29-31 October 2012, Bilbao, Spain.

[6] Gentner C., Sallaberger M., Widmer C., Braun =., Staubli T. (2012) Numerical and experimental analysis of instability phenomena in pump turbines 26th IAHR Symposium on Hydraulic Machinery and Systems 15 (2012) 032042 doi:10.1088/1755-1315/15/3/032042

Fig.17 Wavelet magnitude of the pressure signal at the leading edge in the wickets gates channel vane for 0.63 Q_{Des} (a), 0.60 Q_{Des} (b) and 0.58 Q_{Des} (c).

[7] Guo S., Maruta Y. (2005) Experimental investigations on pressure fluctuations and vibration of the impeller in a centrifugal pump with vaned diffusers. JSME Int. J., Ser. B, 48(1), pp. 136–143.

[8] Henry J.M., Houdeline J.B., Ruiz S., Kunz T. (2012) How reversible pump-turbines can support grid variability - The variable speed approach. HYDRO 2012 Innovative Approaches to Global Challenges, 29-31 October 2012, Bilbao, Spain.

[9] Hui Sun; Ruofu Xiao; Weichao Liu; Fujun (2013) Wang Analysis of S Characteristics and Pressure

Pulsations in a Pump-Turbine With Misaligned Guide Vanes, J. Fluids Eng.. 2013; 135(5), 051101-051101-6. FE-12-1122, doi: 10.1115/1.4023647.

[10] Li Deyou, Wang Hongjie, Xiang Gaoming, Gong Ruzhi, Wei Xianzhu, Liu Zhansheng (2015) Unsteady simulation and Analysis for hump characteristics of a pump turbine model, Renewable Energy, 77 (2015), pp. 32-42, DOI: 10.1016/j.renene.2014.12.004.

[11] Li, W. (2012) Numerical investigation of pump-turbines with different blades at pump conditions, Journal of advanced manufacturing systems [0219-6867] vol:11(2), pp 143-153.

[12] Iino M, Tanaka K. (2004) Numerical analysis of unstable phenomena and stabilizing modification of an impeller in a centrifugal pump. In: Proceedings of 22nd IAHR symposium on hydraulic machinery and systems. Stockholm, Sweden; 2004.

[13] Liu JT, Liu SH, Wu YL, Jiao L, Wang LQ, Sun YK. (2012) Numerical investigation of the hump characteristic of a pump-turbine based on an improved cavitation model. Comput Fluids 2012 (68), pp. 105-11.

[14] Minemura, K., Murakami, M. (1980): A Theoretical Study on Air Bubble Motion in a Centrifugal Pump Impeller, Proc. ASME/JSME Fluid Eng. Conf., Fed-Vol. 102, pp. 446-455

[15] Pavesi G., Cavazzini G., Ardizzon G. (2008) Time–frequency characterization of the unsteady phenomena in a centrifugal pump. Int. J. Heat Fluid FL, 29, pp. 1527–1540, DOI: 10.1016/j.ijheatfluidflow.2008.06.008

[16] Pavesi G., Cavazzini G., Ardizzon G. (2008) Time-frequency characterization of rotating instabilities in a centrifugal pump with a vaned diffuser, International Journal of rotating Machinery, Vol. 2008 , DOI: 10.1155/2008/202179

[17] Pavesi G., Cavazzini G., Jun Yang, Ardizzon G. (2014) Flow Phenomena Related to the Unstable Energy-Discharge Characteristic of a Pump-Turbine in Pump Mode 15th International Symposium on Transport Phenomena and Dynamics of Rotating Machinery, ISROMAC-15 February 24 - 28, 2014, Honolulu, HI, USA.

[18] Rodriguez C.G., Egusquiza E, and Santos IF (2007) Frequencies in the vibration induced by the rotor stator interaction in a centrifugal pump turbine. J. Fluids Eng., 129(11), pp. 1428–1435, DOI: 10.1115/1.2786489.

[19] Rodriguez C.G., Mateos-Prieto B, and Egusquiza E Monitoring of Rotor-Stator Interaction in Pump-Turbine Using Vibrations Measured with On-Board Sensors Rotating with Shaft, Shock and Vibration, Volume 2014 (2014), Article ID 276796.

[20] Rosenblatt M., Van Ness J.W. (1965) Estimation of the Bispectrum. Ann. Math. Stat., vol. 36, pp. 1120-1136

[21] Torrence C., Compo G., (1998) A practical guide to wavelet analysis. Bull. Am. Meteorol. Soc. 79 (1), pp. 61–78.

[22] Yan J., Koutnik J., Seidel U., Hubner B. (2010) Compressible simulation of rotor-stator interaction in pump-turbines. In: Proceedings of 25th IAHR symposium on hydraulic machinery and systems, Timisoara, Rumania; 2010.

[23] Yang J, Pavesi G, Cavazzini G, Yuan S (2013) Numerical characterization of pressure instabilities in a vaned centrifugal pump under part load condition. IOP Conf. Ser.: Mater. Sci. .Eng. 52 0022044, 6th International Conference on Pumps and Fans with Compressors and Wind Turbines (ICPF2013), DOI: 10.1088/1757-899X/52/2/022044.

[24] Yang J., Pavesi G., Yuan S., Cavazzini G., Ardizzon G. (2015) Experimental characterization of a pump-turbine in pump mode at hump instability region, Renewable Energy, Vol 137,(4) (2015), DOI: 10.1115/1.4029572

[25] Yuekun Sun, Zhigang Zuo, Shuhong Liu, Jintao Liu, and Yulin Wu (2014) Distribution of Pressure Fluctuations in a Prototype Pump Turbine at Pump Mode, Advances in Mechanical Engineering Volume 2014, Article ID 923937.

FUNDING